Authors: James R. Collins[1,2*†], Paul D. Fucile[3], Glenn McDonald[4], Justin E. Ossolinski[2], Richard G. Keil[5], James R. Valdes[3], Scott C. Doney[2], and Benjamin A. S. Van Mooy[2*]

Title: An autonomous, *in situ* light-dark bottle device for determining community respiration and net community production

Affiliations: [1] MIT/WHOI Joint Program in Oceanography/Applied Ocean Science and Engineering, Woods Hole, Massachusetts, USA

[2] Department of Marine Chemistry and Geochemistry, Woods Hole Oceanographic Institution, Woods Hole, Massachusetts, USA

[3] Department of Physical Oceanography, Woods Hole Oceanographic Institution, Woods Hole, MA 02543, USA

[4] Department of Applied Ocean Physics and Engineering, Woods Hole Oceanographic Institution, Woods Hole, MA 02543, USA

[5] School of Oceanography, University of Washington, Seattle, WA 98195, USA

*** Correspondence:** James R. Collins, james.r.collins@aya.yale.edu or Benjamin A. S. Van Mooy, bvanmooy@whoi.edu

† Present Address: James R. Collins, School of Oceanography and eScience Institute, University of Washington, Seattle, WA 98195, USA

Running head: Autonomous observations of community metabolism

Keywords: respiration, community metabolism, aquatic microbial ecology, autonomous instrumentation, optodes, dissolved oxygen, ocean observing

Abstract

We describe a new, autonomous, incubation-based instrument that is deployed *in situ* to determine rates of gross community respiration and net community production in marine and aquatic ecosystems. During deployments at a coastal pier and in the open ocean, the PHORCYS (*PHO*tosynthesis and *R*espiration *C*omparison-*Y*ielding *S*ystem) captured dissolved oxygen fluxes over hourly timescales that were missed by traditional methods. The instrument uses fluorescence-quenching optodes fitted into separate light and dark chambers; these are opened and closed with piston-like actuators, allowing the instrument to make multiple, independent rate estimates in the course of each deployment. Consistent with other studies in which methods purporting to measure the same metabolic processes have yielded divergent results, respiration rate estimates from the PHORCYS were systematically higher than those calculated for the same waters using a traditional two-point Winkler titration technique. However, PHORCYS estimates of gross respiration agreed generally with separate incubations in bottles fitted with optode sensor spots. An Appendix describes a new method for estimating uncertainties in metabolic rates calculated from continuous dissolved oxygen data. Multiple successful, unattended deployments of the PHORCYS represent a small step toward fully autonomous observations of community metabolism. Yet the persistence of unexplained disagreements among aquatic metabolic rate estimates — such as those we observed between rates calculated with the PHORCYS and two existing, widely-accepted bottle-based methods — suggests that a new community intercalibration effort is warranted to address lingering sources of error in these critical measurements.

Introduction

Accurate, reproducible, and cost-effective estimates of aerobic respiration and primary production in aquatic systems are essential for research across a diverse array of disciplines in the environmental sciences (del Giorgio and Williams, 2005; Volkmar and Dahlgren, 2006; Staehr et al., 2012). Rate measurements of these two metabolic parameters can be applied to various problems, including validating the biogeochemical components of global climate models (Denman et al., 2007), determining the trophic status of surface-water planktonic communities in open ocean ecosystems (Williams, 1998), measuring rates of biological oxygen demand (BOD) in treated wastewater (Spanjers et al., 1994), and identifying unexpected metabolisms in the deep ocean (Reinthaler et al., 2010).

While an increasing demand for metabolic rate data has encouraged the development of many different methods for estimating rates of photosynthesis (Ducklow and Doney, 2013), the number of new methods for measuring aerobic respiration at the community scale has lagged behind considerably (del Giorgio and Williams, 2005). The majority of field-based methods for measuring rates of respiration and primary production in the ocean fall largely into two categories: (1) *in situ* geochemical tracer techniques that track changes in the concentration or isotopic composition of dissolved oxygen and carbon dioxide within ocean water masses (e.g., the surface mixed layer), and (2) *in vitro* incubation techniques that track the rates at which plankton exchange oxygen or carbon dioxide in discrete seawater samples (i.e., bottle incubations). The merits and faults of these two categories of approaches have been vigorously debated while significant and often unexplained differences are noted in the rate estimates they yield (Duarte et al., 2013; Ducklow and Doney, 2013; Williams et al., 2013). The former category has benefited considerably from recent advances in optical sensor technology (Moore et al., 2009), mass spectrometry (Goldman et al., 2015), and techniques for analysis of optical sensor data from autonomous underwater vehicles (Nicholson et al.,

2015). By maximizing the extent to which sensors are integrated into the surrounding environment, low-power instruments increase the spatial and temporal resolution of geochemical tracers *in situ* and permit increasingly autonomous, long-term deployments (Prien, 2007; Riser and Johnson, 2008; Porter et al., 2009).

By contrast, the field has seen relatively few technical advances in *in vitro* incubation techniques. *In vitro* techniques provide an important complement to *in situ* methods because they are sensitive to short-term perturbations and are amenable to experimental design. For these reasons, the traditional two-point light and dark bottle incubation technique (Gaarder and Gran, 1927) and the ^{14}C incubation method (Steeman Nielsen, 1952) continue to dominate incubation-based studies, although a number of other methods based on electron transport (e.g., Kenner and Ahmed, 1975) or fluxes of ^{18}O or CO_2 (Bender et al., 1987; Robinson and Williams, 2005) have been introduced over the course of the last half-century. A number of these methods have been incorporated into modern designs for benthic flux chambers and so-called "benthic landers," enabling investigators to capture fluxes of oxygen and other gases *in situ* at the sediment-water interface instead of in core samples aboard ship (Hammond et al., 2004; compare, e.g., Martens et al., 2016, Fuchsman et al., 2015, or Lee et al., 2015, to Kim et al., 2015). However, even the most advanced of these devices can require the use of divers or remotely operated vehicles (ROVs) for deployment, maintenance, or recovery. Additionally, by their nature, few of these designs can be programmed to conduct multiple incubations over the course of a single deployment. Taylor et al. addressed this obstacle with the submersible incubation device (SID), which for the first time allowed multiple, unattended incubations with ^{14}C-bicarbonate to be conducted *in situ* (Taylor and Doherty, 1990; Taylor et al., 1993). The SID represented a significant advance but was limited by its relatively small 400 mL incubation chamber and its reliance on the use of radiolabeled reagents.

Among the advances most consequential for *in situ* instrumentation was the adaptation to marine applications of optical technologies such as optodes (e.g., Klimant et al., 1995; Tengberg et al., 2006) and optode sensor spots (e.g., Warkentin et al., 2007), which exploit fluorescence (luminescence) quenching to measure dissolved oxygen concentrations non-destructively and without themselves contributing to oxygen consumption in the sample. Integral optodes and sensor spots based on the same technology have now been successfully used in a variety of shipboard configurations to measure rates of gross community respiration in whole, unconcentrated and unfiltered water samples and in water containing particle material from marine and aquatic environments (Edwards et al., 2011; Wikner et al., 2013; Collins et al., 2015). More recently, shipboard *in vitro* measurements of respiration within individual marine particles were made successfully using oxygen microelectrodes (Belcher et al., 2016a; Belcher et al., 2016b). A significant recent advance was also achieved with the RESPIRE device, which uses an optode fitted into a modified sediment trap to make particle respiration measurements *in situ* (Boyd et al., 2015; McDonnell et al., 2015).

Despite the significant progress represented in these optode-driven systems, incubation-based methods remain prone to a number of sources of error that demand reconciliation. These can be generally divided into two categories: (1) those that result from the preparation for or act of incubating natural microbial populations and (2) errors inherent in the method used to determine the concentration of dissolved oxygen (e.g., Winkler titration, fluorescence-quenching optode, or Clark electrode). The sources of uncertainty associated with bottle/chamber incubations span both categories and include (1) contamination, disruption, or bias introduced through the process of obtaining seawater samples from depth and preparing them for incubation (Suter et al., 2016; Tamburini et al., 2013); (2) unrepresentative incubation conditions that do not faithfully reproduce the variations in temperature, turbulence, and light inherent in natural systems; (3) so-called “bottle

115 effects" associated with low-volume incubations which may limit nutrient availability (Furnas, 2002)
116 or induce unnatural changes in community structure (Venrick et al., 1977; Calvo-Díaz et al., 2011);
117 and (4), in the case of metabolic rate measurements extrapolated from Winker (1888) titrations, the
118 lack of temporal resolution inherent in measurements based only on two endpoints. In any study
119 where incubations are used, the choice of incubation methodology places inherent limits on the
120 spatial and temporal resolution of the data collected (Karl et al., 2001). The integration of point
121 measurements — data sparse in time and/or space, whether based on *in situ* observations or
122 incubations — also creates significant representation error. One solution to this problem is to greatly
123 increase the number of measurements made during data collection using automated technologies.

124 We describe here the *PHO*tosynthesis and *R*espiration *C*omparison-*Y*ielding *S*ystem
125 (PHORCYS), a large-volume (i.e., > 2.5 L), light and dark chamber incubation system for
126 autonomous measurement of rates of primary production and respiration at high temporal resolution
127 and under *in situ* conditions. In designing the instrument, we endeavored to minimize the major
128 hypothesized sources of uncertainty associated with traditional incubation-based methods while
129 constructing a system that functions autonomously and interrogates water samples non-destructively.
130 We also sought to eliminate or reduce the need for repeated wet-chemical field measurements such as
131 Winkler oxygen titrations or reagent-based methods used in other autonomous systems. We first
132 describe design and validation of the PHORCYS using two independent methods, and then present
133 results of several deployments of the instrument in different ecosystem types.

134 **Materials and procedures**

135 *Instrument design and operation*

136 The PHORCYS is composed of only a few basic components, making the design highly
137 scalable and cost-effective (Fig. 1a,b). In nearly all instances, "off the shelf" components of different

size or capacity can be easily substituted for those we describe here. The PHORCYS consists of two polycarbonate plastic chambers (usable vol. 5.7 L; Table 1), several auxiliary sensors for collection of environmental data in the ambient water mass outside the chambers, and a watertight power supply, control, and data recording module (Fig. 1a). A piston-like, magnetically coupled actuator is programmed to open and close each chamber at a specified interval, allowing users to perform multiple, unattended incubations over the course of a single deployment. The chamber seals are tapered to avoid the use of rubber O-rings that might have introduced a source of organic contamination into the sample water. In experiments, the polycarbonate plastic used for the PHORCYS incubation chambers reduced photosynthetically active radiation (PAR) within the transparent chamber to 83% of incident strength; we present a means of accounting for this attenuation, below. The opaque chamber was darkened by application of a coating to the outside of the cylinder. All PHORCYS components are mounted to a stainless-steel frame, allowing the instrument to operate to a depth of 100 m.

Dissolved oxygen concentrations in the two chambers are monitored with fast-response, fluorescence quenching oxygen optodes (Aanderaa model 4531D; accuracy < 8 μM O_2; resolution < 1 μM O_2; response time < 30 s; Aanderaa Data Instruments, Inc., Bergen, Norway); each optode is fitted into its chamber using a water- and gas-tight flange assembly. The instrument also has several external sensors, including a third optode to monitor dissolved oxygen concentrations in the water mass outside of the two chambers, PAR sensor, beam transmissometer, chlorophyll fluorometer, and CTD. We did not investigate whether the arrangement of these sensors had any effect on the external dissolved oxygen field surrounding the instrument.

With a full sensor suite, the nominal power consumption of the PHORCYS is 50 mA at 12V; standby current is 2 mA. When programmed to sample at a 50 % duty cycle, a single 12V primary ‘D’ cell battery pack (20,000 mAh capacity) will power the instrument for up to 30 d in an

unattended deployment mode. Data are recorded in an ASCII fixed-field format onto a micro SD card in a DOS-readable format. For attended deployments, a combination communications and external power port provides the ability to observe data in real time, allow program updates, download data, and power the instrument indefinitely. The sampling interval is nominally set to 1 min, though data can be collected as frequently as every 15 s. The acquisition program determines sampling activity by way of a real-time clock. The chambers can thus be programmed to open and close at any time, allowing the investigator to make multiple incubations of any desired length. In the configuration used to acquire the data presented here, (Fig. 2, ■ symbol; e.g., Fig. 3) the chambers were programmed to open at or around sunrise and the same operation was repeated at sunset, providing two incubations in each 24 h period that aligned with the beginning and end of the photoperiod. The chambers are opened and then closed sequentially (i.e., one after the other) to reduce total current draw from the power source. The chambers remain open for 30 min at the outset of each incubation, providing sufficient time for the water to be fully exchanged before closure; we confirmed this flushing time was sufficient in both quiescent and flowing (~ 1 m s^{-1}) waters using a series of tests with a tracer dye (results not shown). While we used a standard 30 min flush time in the deployments for which data is presented below, any time can be specified in the instrument's control software, which is written in BASIC.

The earlier PHORCYS data from 2012 (Fig. 2, ● symbols; e.g., Fig. 4) were obtained using a prototype instrument that permitted only one incubation cycle per deployment. This prototype (Fig. 1b) was assembled from two 2.5 L Niskin-style sampling bottles mounted to an aluminum frame (opaque polyvinylchloride and transparent polycarbonate plastic, respectively; actual usable volume, 2.6 L; General Oceanics, Inc., Miami, FL, USA). Closure of the chambers for incubation was effected using an electrolytic time release (i.e., "burn wire") system. Prior to deployment, the Niskin bottle endcaps were cocked open and the retaining cable was rigged to a fusible burn wire plug. Once

186 in the water, a sufficient current was applied to the burn wire at a time set by the user, corroding the
187 wire and allowing the bottle endcaps to close. The chambers were then sealed and the incubation
188 began. For the deployments presented here, we programmed the chambers to close approximately 45
189 min after the PHORCYS had reached the desired depth. In the prototype instrument, Aanderaa model
190 4330F optodes (accuracy < 8 μM O_2; resolution < 1 μM O_2) were used to record dissolved oxygen
191 concentrations.

192 *Instrument deployments*

193 We conducted 6 unattended deployments of the PHORCYS in 3 distinct ecosystem types in
194 the North Atlantic basin (Fig. 2; Table 2; Supplemental Table 1). Open-ocean deployments (2 to 7 d
195 in length, using the prototype instrument) were conducted during cruises aboard the R/V *Knorr*;
196 during these deployments, the instrument was suspended at various depths in the euphotic zone from
197 a drifting surface buoy (Fig. 1c). Deployment and recovery were accomplished in 45-60 min from a
198 standard oceanographic research platform (Supplemental Fig. 1). An Argo satellite beacon (Fig. 1c)
199 allowed us to track the array remotely between deployment and recovery while the ship traveled up
200 to 300 km away to conduct other shipboard scientific operations; we specifically designed both
201 models of the PHORCYS to be wholly autonomous, incurring a minimal burden on other shipboard
202 operations. Pierside deployments were conducted using the present, multiple-incubation version of
203 the PHORCYS at the Iselin Marine Facility, Woods Hole, MA, USA (41º 31' 24" N 70º 40' 20" W);
204 the site adjoins a highly productive coastal embayment. In both cases, oxygen concentrations (μmol
205 L^{-1} O_2), percent saturation, and temperature were then recorded for each chamber at 1 min intervals.
206 Post-acquisition corrections for salinity were applied to both the open-ocean and coastal data using
207 concurrent observations of salinity and manufacturer-supplied correction coefficients. Concurrent
208 salinity data were obtained from the continuous, flow-through CTD system aboard the R/V *Knorr*
209 (for open-ocean deployments) or from the Seabird CTD unit mounted as an external sensor on the

present PHORCYS model (2016 coastal deployments). Due to the limited number of at-sea deployments of the PHORCYS prototype and the challenges we encountered during our initial cruises, we pooled our prototype results with the data we later obtained from the production-model instrument in order to assemble a larger, more robust dataset for subsequent analysis.

Instrument calibration and choice of deployment depth

Optodes were calibrated before each pierside deployment and prior to each research cruise using a two-point method, assuming a linear response between end-members. An air-saturated solution was obtained according to manufacturer instructions by bubbling ambient air for approx. 30 min through a sufficient volume of Milli-Q water using an aquarium stone; a zero-oxygen solution was obtained by dissolving an excess of reagent-grade sodium sulfite into a beaker containing Milli-Q water. The optodes were then calibrated at atmospheric temperature and pressure, as recommended by the manufacturer. At the open-ocean stations, we deployed the prototype instrument within the euphotic zone at depths where the observed flux of photosynthetically active radiation (PAR; wavelengths 400-700 nm) was between 10-30% of the incident flux at the surface. The depth of the euphotic zone (z_{eu}, defined as the depth at which PAR = 1 % of incident intensity) was identified using profiles from shipboard hydrocasts. At each of these stations, we calculated an equivalent deployment depth (z_{equiv}) that accounted for light attenuation by the transparent chamber's polycarbonate plastic, according to a modification of the standard equation for the exponential decay of light with depth:

$$I_z(PAR) = \frac{I_0(PAR)e^{-K_d(PAR)z_{equiv}}}{T(PAR)} \qquad (1)$$

where $I_0(PAR)$ and $I_z(PAR)$ are, respectively, the incident PAR intensity and intensity at depth z, $K_d(PAR)$ is the diffuse attenuation coefficient for the PAR spectral band (calculated from the

hydrocast profile at each station), and $T(PAR)$ is the transmissivity of the polycarbonate plastic expressed as a fraction (0.83). Pierside deployments of the present PHORCYS model were conducted at a depth of 1.5 m.

Instrument validation by two independent methods

First, to validate the optodes' ability to accurately track respiration, we used a standard analytical method — two-point Winkler titration — to determine dissolved oxygen consumption in triplicate water samples at the beginning and end of each incubation period (present model instrument) or deployment (for data obtained with the prototype). Winkler titrations were conducted in 125 mL BOD bottles according to EPA Method 360.2 as modified for shipboard determination in seawater (Knapp et al., 1989). Initial Winkler titrations were made in samples collected within 15 min of deployment using a Niskin or Go-Flo bottle suspended at the same depth as the instrument. A set of three darkened 125 mL BOD bottles containing water from the same Niskin or Go-Flo bottle was incubated at *in situ* temperature until the PHORCYS was recovered or the incubation period ended; these samples were then sacrificed according to the same protocol. The BOD bottles used in these incubations were triple-rinsed with 10 % HCl and then Milli-Q water prior to sampling. All reagents for Winkler titrations were A.C.S. grade or better; the sodium thiosulfate titrant was standardized daily. Amperometric titration was performed using an autotitrator (Metrohm 904 Titrando; Metrohm USA, Inc., Riverview, FL).

As an additional means of comparison during the open-ocean deployments, we also tracked changes in dissolved oxygen in a series of continuously monitored shipboard bottle incubations. Water from the PHORCYS deployment depth was retrieved for these incubations from a hydrocast made within 1 h of deployment. Incubations were conducted in gas-tight, 300 mL glass BOD bottles; at least 5 replicates were used for each series of measurements. Determination of dissolved oxygen

was made at 3 to 9 h intervals using optode spot minisensors (PreSens PSt3; response time < 40 s; Precision Sensing GmbH, Regensburg, Germany; Warkentin et al., 2007) that were glued to the inside surfaces of the bottles using food-quality silicone cement. The use of these optode spots eliminated the need for drawing of aliquots from the sample bottles; the bottles had been soaked in Milli-Q water for > 2 months following application of the sensor spots. Incubations were conducted in the dark at *in situ* temperature as described in Edwards et al. (2011).

Data analysis

PHORCYS rate calculations

Volumetric rates of gross community respiration (GR) and net community production (NCP) were calculated by linear least-squares regression of observations of dissolved oxygen concentration over the length of the deployment (prototype model) or incubation period (present model). We assumed the only significant chemical reactions contributing to oxygen consumption and evolution in the two chambers were aerobic respiration and photosynthesis. For organic matter of elemental stoichiometry roughly corresponding to that of Redfield (1934) and assuming production is based on nitrate, these redox reactions can be represented as (after Stumm and Morgan, 2013):

$$138O_2 + C_{106}H_{263}O_{110}N_{16}P + 18HCO_3^- \rightarrow 124CO_2 + 16NO_3^- + HPO_4^{2-} + 140H_2O \quad (2)$$

and

$$106CO_2 + 16NO_3^- + HPO_4^{2-} + 122H_2O + 18H^+ + h\nu \rightarrow C_{106}H_{263}O_{110}N_{16}P + 138O_2 \quad (3)$$

As is the case with the classic light and dark bottle incubation technique, we assumed that only respiration was taking place in the dark (i.e., GR; reported as positive quantities), while both reactions were taking place simultaneously in the presence of light (i.e. NCP; in reality,

276 photorespiration also contributes to oxygen consumption in the light bottle). Finally, where possible,
277 we estimated the rate of gross primary productivity (GPP) according to the relationship

278 $$\mathrm{GPP} = \mathrm{NCP} + \mathrm{GR} \qquad (4)$$

279 To estimate uncertainties in PHORCYS rate estimates, we adapted an effective degrees of freedom
280 technique traditionally applied to time-series data in physical oceanography (Emery and Thomson,
281 2001). The method, which serves as an alternative to the standard error of the regression slope in
282 instances when true replication cannot be achieved, is described in detail in the Appendix.

283 *Rate calculations from Winkler titration samples and sensor spot incubations*

284 For the Winkler titration samples, GR was calculated using a difference of means,

285 $$\mathrm{GR} = -\frac{d\mathrm{O}_2}{dt} \qquad (5)$$

286 where $d\mathrm{O}_2$ is the difference between the mean dissolved oxygen concentration in samples sacrificed
287 at the final incubation timepoint and the mean measured at the initial timepoint and dt is the
288 incubation duration. For the sensor spot incubations, we calculated rates for each bottle using a linear
289 least-squares regression of all observations recorded over the time period; we then averaged the rates
290 obtained for the various replicates to obtain a final estimate. Uncertainties in rates based on the
291 Winkler titration method were determined from the standard deviations of the dissolved oxygen
292 concentrations measured in the replicates at each timepoint. For rates based on the sensor spot
293 incubations, we used the standard error of regression. While we report metabolic rate estimates from
294 the PHORCYS in oxygen-based units, a stoichiometric relationship such as the molar respiratory
295 quotient of Anderson and Sarmiento (1994) can be applied to convert these estimates to units of
296 carbon.

Assessment

PHORCYS metabolic rate estimates

We observed a significant degree of daily and hourly variability in the time series data from each PHORCYS deployment (e.g., Fig. 3 and 4). This variability manifested itself in a wide range of metabolic rate estimates (Table 2; Supplemental Table 1) that reflect the interaction of multiple biological and physical forcings, including diel changes in cellular growth cycle, surface-layer water temperature, and irradiance. Daily rates of GR were estimated from dark chamber data for all PHORCYS deployments (Table 2). For data obtained with the present model instrument, hourly rates were calculated for each incubation segment (Fig. 3); these were extrapolated to daily rates to facilitate comparison with other studies and with data from the prototype instrument. For open-ocean data obtained with the PHORCYS prototype, daily rates were calculated using the entire DO time series from each deployment. Erroneous readings from one of the optodes and a system malfunction prevented us from recovering usable NCP data from the transparent chamber during two of the open-ocean deployments of the prototype instrument. During the 24-27 April 2012 deployment, the chosen depth of 29 m provided insufficient PAR (< 3% of surface intensity) to support measurable photosynthesis in the transparent chamber; consequently, we could not calculate NCP or GPP for this station (Supplemental Table 1). An obstruction prevented the transparent chamber from closing during the November 2016 deployment, allowing us to recover useful data from only the dark chamber.

We captured daily rates of GR ranging from 1.8 ± 0.2 μmol O_2 L^{-1} d^{-1} at a mid-latitude station in the North Atlantic to 10.5 ± 7.5 and 18.9 ± 1.9 μmol O_2 L^{-1} d^{-1} in two different water masses at the Woods Hole pier in early November (Fig. 3 and 4; Table 2). The wide variation in GR we observed with the PHORCYS covers a significant range of the rates for marine systems compiled

by Robinson and Williams (2005). Daily rates of GPP at the PHORCYS deployment depth ranged from essentially zero on several days at a mid-latitude station in the North Atlantic (Supplemental Table 1) to 3.6 ± 0.5 μmol O_2 L^{-1} d^{-1} during a coccolithophore bloom (Collins et al., 2015) in the sub-Arctic North Atlantic (Fig. 4). Rates of NCP at the deployment depth ranged from –2.0 ± 0.4 μmol O_2 L^{-1} d^{-1} to –4.2 ± 0.2 μmol O_2 L^{-1} d^{-1} (Supplemental Table 1).

Discussion

Subdaily variation in rates of metabolism; choices concerning data analysis

Increasing evidence suggests the significant sub- and inter-daily variation in metabolic activity captured by the PHORCYS exists in almost all natural aquatic systems (Caffrey, 2004; Staehr et al., 2012; Collins et al., 2013); even in oligotrophic waters, respiration and production rates may change significantly from one day (or hour) to the next, even as the system maintains an overall state of near trophic balance (Aranguren-Gassis et al., 2012). The types of fluctuations we observed in the various dissolved oxygen time series obtained from the PHORCYS appear to be characteristic of incubation-based *in situ* instruments. McDonnell et al. (2015) and Boyd et al. (2015) both observed similar patterns in dissolved oxygen data during recent deployments of an *in situ* device that measures oxygen consumption rates on marine particles.

Nevertheless, the subtle changes in DO concentration we observed in multi-day incubations with the PHORCYS prototype (e.g., Fig. 4) suggest that a single regression line — fitted, in this case, to align with the closing and opening of the chambers — might have been poorly suited to a time series exhibiting such variation. While one might instead have divided the full time series into shorter segments to compute several different regressions (e.g, according to the photoperiod), we chose to define the interval for rate calculations from the prototype instrument according the chamber opening and closing times. This allowed us to avoid the bias inherent in dividing such a time series into

343 smaller segments. The present PHORCYS model allows users to predefine multiple, shorter
344 incubation periods of length appropriate to the ecosystem (e.g., Fig. 3); this feature eliminates the
345 need for a choice between either a subjective, *ex post facto* division of data or the application of a
346 single regression that might fail to capture the observed variation.

347 *Evaluation of instrument performance using independent methods*

348 PHORCYS estimates of community respiration were systematically higher than those
349 calculated for the same waters using the two-point Winkler titration method (Fig. 5a; Table 2). While
350 there was a significant correlation between estimates from the two different methods ($r^2 = 0.42$; $p =$
351 0.04), the traditional Winkler titration approach appeared to underestimate rates of respiration by
352 nearly one-third. Alternatively, the PHORCYS could have overestimated true rates of respiration
353 through artificial stimulation of the microbial community or inadvertent retention of residual
354 dissolved oxygen by the chambers or optode. In contrast, rate estimates from the PHORCYS
355 generally agreed with those based on our non-destructive optode sensor spot incubations, though we
356 had only five data points on which to evaluate the correlation (Fig. 5b; correlation was not
357 statistically significant).

358 Wikner et al. (2013) observed close agreement (~ 3 % deviation) between gross community
359 respiration rates derived from continuous optode measurements in a shipboard incubation chamber (1
360 L, clear glass) and a series of parallel incubations based on a Winkler method in 120 mL glass BOD
361 bottles. In previous work, we observed similar coherence between rates derived from a two-point
362 Winkler method in 300 mL glass BOD bottles and those based on incubations in 125 mL glass BOD
363 bottles fitted with optode sensor spots (surface area : volume ratios as reported in Table 1; Collins et
364 al., 2015). Underlying the agreement among methods in these previous studies is a common reliance
365 on incubations aboard ship. One might therefore conclude that the observed divergence between

366 estimates of respiration from the PHORCYS and those we made with the Winkler titration method
367 are due to inherent differences between the *in situ* PHORCYS approach and shipboard incubation
368 methods. However, evidence suggests that use of the same method is not even a guarantor of
369 agreement. For example, Robinson et al. (2009) found that vastly different rates were obtained from
370 the same method of measuring primary production when the only the timescale of incubation was
371 varied.

372 *Possible sources of observed discrepancies between methods*

373 *Gas permeability of materials*

374 The materials chosen for construction of the PHORCYS, particularly the polycarbonate
375 plastic we used for the incubation chambers, represent one possible source of bias in our method. We
376 chose polycarbonate material for its durability, low cost, and, compared with other plastics such as
377 polyvinylchloride, minimal biological reactivity. Polycarbonate was selected for its minimal
378 biological reactivity in construction of at least two similar *in situ* incubation devices (Langdon et al.,
379 1995; Robert, 2012). However, polycarbonate, like most plastics, is at least partially permeable to
380 dissolved oxygen; by comparison, the borosilicate glass of which BOD bottles are fabricated is
381 nearly impermeable (Kjeldsen, 1993; Robert, 2012). While some diffusion of dissolved oxygen
382 across the polycarbonate chamber walls could have occurred during incubations with the PHORCYS,
383 thus biasing our results, we believe the effect would likely have been very modest given the
384 dissolved oxygen gradients and timescales typical of our deployments. First, the gradient necessary
385 to drive any diffusion across the PHORCYS chamber wall (i.e., the difference between the internal
386 and external dissolved oxygen concentrations) did not exceed 25 μmol O_2 L^{-1} during any
387 deployment; in the deployment presented in Fig. 3, the average difference between internal and
388 external concentrations was just 6.1 μmol O_2 L^{-1}. In a series of oxygen-diffusion experiments with a

389 device similar to the PHORCYS, Robert (2012) monitored the dissolved oxygen concentration inside
390 a polycarbonate chamber after the water inside was treated with sodium hydrosulfite to render it
391 anoxic. After manipulating the dissolved oxygen concentration in water outside the chamber to create
392 cross-boundary gradients ranging from approx. 50 μmol O_2 L^{-1} to > 350 μmol O_2 L^{-1}, the authors
393 observed little change in the dissolved oxygen concentration inside the chamber on timescales similar
394 to those of the PHORCYS deployments (11-12 h for the current version of the instrument; 3-5 d for
395 the PHORCYS prototype). Further, in a comprehensive study of the permeabilities of several gases
396 (O_2, N_2, CO_2, and CH_4) in various polymers, Kjeldsen (1993) concluded that bias introduced by
397 permeability should be taken into account primarily when certain materials such as silicone rubber
398 were considered for use in anoxic waters; silicone rubber is more than 250 times as permeable to
399 dissolved oxygen than the polycarbonate plastic we used in construction of the PHORCYS (Kjeldsen,
400 1993).

401 *Handling or sampling bias*

402 Errors or bias introduced during the handling and manipulation of samples for bottle
403 incubations might also explain some of the discrepancy in rate measurements. For example, the
404 PHORCYS minimizes physical disturbances associated with seawater handling: Since the instrument
405 takes seawater samples and then incubates them in place, the planktonic community is not subjected
406 to rapid changes in temperature, pressure, and light associated with bringing water samples to the
407 surface via hydrocast and preparing them for shipboard incubations (Calvo-Díaz et al., 2011). The
408 PHORCYS also minimizes another potential bias that can arise when water containing marine
409 microbes is sampled from Niskin bottles; Suter et al. (2016) found that variation in settling rates
410 among marine particles can lead to an undersampling of microbial communities on faster-sinking
411 particles, which can fall below the bottles' spouts before aliquots can be drawn.

412 *Biofouling and surface colonization*

413 While we did not observe any significant biofouling of the PHORCYS or its components
414 during the deployments for which data are presented here, unwanted biological growth represents a
415 significant challenge and source of potential bias when autonomous sensors are deployed in the
416 surface and mesopelagic ocean (Delauney et al., 2010; Manov et al., 2004; e.g., Collins et al., 2013).
417 We imagine biofouling could represent a significant obstacle during future deployments if the
418 deployment duration were to exceed 5-7 d (the maximum explored in this work; Table 2), or if the
419 instrument were deployed in a productive ecosystem during a period of elevated primary production.
420 Compare, however, Robert (2012), who reported little biofilm growth on the chamber of a similar
421 incubation-based instrument after deploying it with no fouling controls for several months in the
422 Mediterranean Sea.

423 The lack of visual evidence of fouling in the PHORCYS chambers notwithstanding, there is
424 substantial evidence that microbial colonization of surfaces happens rapidly in the marine
425 environment (Salta et al., 2013; Dang and Lovell, 2016). It is therefore almost certain that at least
426 some microbial colonization of the chamber walls would have taken place within the 3-5 d timescale
427 of our deployments. Because we did not make measurements of biofilm activity or species
428 abundance, it is impossible to diagnose what contribution these communities might have made to the
429 observed fluxes in dissolved oxygen. However, compared to the surface area to volume ratios of the
430 150 and 300 mL vessels in which the other rate measurements were made (125 mL bottle, 0.83; 300
431 mL bottle, 0.77), the lower surface area to volume ratios of the PHORCYS chambers (current model,
432 0.34; prototype, 0.67) provide fewer opportunities for colonization relative to the volume being
433 incubated (Table 1). There is also some evidence that the small volumes typical of BOD bottles may
434 induce non-representative changes in the planktonic microbial community during incubations on
435 timescales of 24-48 h (Pratt and Berkson, 1959); however, compare Fogg and Calvario-Martinez

436 (1989), who found that such bottle size effects were only significant during periods of very high
437 primary productivity. A thorough, systematic assessment of these so-called wall and bottle effects
438 should be part of the community intercalibration we advocate in our conclusion.

439 *Other possible sources of bias*

440 Alternatively, the well-documented dependence of community respiration rates on
441 temperature (Yvon-Durocher et al., 2012) might explain the apparent disagreement between methods.
442 While temperatures within the PHORCYS chambers fluctuated only according to the movement of
443 tidal water masses (Fig. 3) or the natural warming and cooling of the surface layer (Fig. 4), the
444 temperature inside the incubator in which the Winkler samples were kept during the shipboard
445 deployments fluctuated during each series of experiments by ± 2°C from the target. A further, more
446 intriguing explanation for the systematic discrepancy — pointing in this case to overestimation of
447 rates by the PHORCYS — is that dissolved oxygen could have accumulated on the optodes or inside
448 walls of the instrument chambers over the course of each deployment, in spite of the standard 30 min
449 flushing protocol. Wikner et al. (2013) offer convincing evidence for the accumulation of dissolved
450 oxygen on the optode surface and acrylic (polymethylmethacrylate) stopper used in their shipboard
451 incubation apparatus; the application of a correction factor for this bias reduced apparent rates
452 calculated from the optode time series relative to the Winkler method. We did not evaluate oxygen
453 retention by the polycarbonate plastic material of which the PHORCYS chambers were constructed.

454 The nature of linear regression itself may also play a role in differences observed between the
455 PHORCYS and the Winkler-based method. A least-squares regression line fit to a large set of
456 observations collected at high temporal frequency, such as those obtained from the PHORCYS, is
457 sensitive in some degree to each of those observations. In comparison, a rate calculated from the
458 beginning and ending oxygen concentrations in the two-point Winkler method is necessarily sensitive

459 only to those two observations; if some unrepresentative source of variability is present in just one
460 bottle, the entire measurement can be heavily biased. Regression of data from the PHORCYS thus
461 yields rate estimates which are robust to the sampling bias inherent in point measurements, yet the
462 technique leaves the underlying data intact to be further interrogated for information about natural
463 variability.

464 *The "deep breath" phenomenon*

465 Finally, while not evident in data from the deployments presented in Fig. 3 or 4, we did
466 occasionally observe a sharp initial decrease in dissolved oxygen concentration within the chambers
467 shortly after closure (data not shown). This phenomenon was reported extensively by Robert (2012)
468 during testing of a similar instrument in the Mediterranean Sea, and thus warrants further
469 investigation. The initial "deep breath" observed in these instances could reflect the rapid and
470 preferential utilization by the microbial community of a limited but highly labile fraction of the
471 dissolved organic carbon (DOC) pool within the chamber. Such a phenomenon has been observed
472 frequently in rates of DOC consumption in freshwater systems, where labile carbon is often
473 metabolized at a rapid rate in the initial minutes or hours of an incubation, leading to an apparent
474 decline in metabolic activity once the labile pool has been exhausted and the incubation progresses
475 (del Giorgio and Pace, 2008; Guillemette and del Giorgio, 2011; Guillemette, McCallister, et al.,
476 2013). While we did not directly observe a pronounced initial change in the rate of dissolved oxygen
477 consumption in any of our shipboard optode sensor spot incubations, it is possible that our sampling
478 interval (3 to 9 h; see above) was of insufficient resolution to detect it.

479 **Comments and recommendations**

480 Through autonomous collection of biogeochemical observations at uniquely high temporal
481 frequency, the PHORCYS yields estimates of community metabolic activity while simultaneously

freeing the analyst from the logistical constraints of attended water column sampling and preparation of shipboard incubations. While we could not determine the origin of the systematic discrepancy between the PHORCYS rate estimates and those based on the traditional two-point Winkler method, the instrument's design allows investigators to avoid many of the potential biases associated with bottle incubations that have been previously documented in the literature. The PHORCYS offers a further advantage in that it can be used to collect information over multiple timescales about the metabolic state of marine and aquatic ecosystems at minimal cost and burden to the user. While the mixed-layer deployments we have presented here provided volumetric rates of ecosystem metabolism at a single depth, multiple PHORCYS units could be deployed simultaneously at different depths in the water column as a means of making depth-integrated rate measurements; one could compare these rates to estimates obtained from *in situ* geochemical tracer studies. Future work could also include direct, side-by-side comparison of metabolic rates obtained from the PHORCYS with those from the classic, bottle-based ^{14}C or ^{13}C tracer methods.

In this spirit, we believe a new, community intercalibration effort is warranted to systematically evaluate the many sources of uncertainty in incubation-based measurements of community metabolism. The workshops of the Group for Aquatic Primary Productivity (GAP; Figueroa et al., 2014) could serve as a model for such an effort, which should include comprehensive evaluation of various combinations of incubation chamber materials, types of oxygen sensors, chamber sizes, and incubation durations. Genetic and biogeochemical tools for characterizing the extent, mechanisms, and effects of surface colonization within the incubation chambers would be critical to the success of any such endeavor. We are optimistic such an effort might reveal the causes of longstanding discrepancies such as those we observed between our PHORCYS rate estimates and those we obtained with bottle-based methods.

Acknowledgments

We thank the captains and crews of the R/V *Knorr* and R/V *Clifford Barnes*, Anton Zafereo, Kay Bidle, Bethanie Edwards, Filipa Carvalho, Jared Schwartz, Fiona Hopewell, Gabriel Roy Liguori, Richard Payne, Jason C. Smith, Sujata Murthy, Dave Fisichella, Ed O'Brien, Craig Marquette, Erik Smith, Shawn Sneddon, Richard Butler, Helen Fredricks, David Glover, Oliver Newman, Emily Peacock, Leah Houghton, Matthew Bogard, Olivia De Meo, and Joe Salisbury. Sheri White contributed significantly to early development of the PHORCYS. The comments of two reviewers significantly improved our original manuscript. This research was supported by the U.S. National Science Foundation (awards OCE-1155438 to B.A.S.V.M., J.R.V., and R.G.K., and OCE-1059884 to B.A.S.V.M.), the Woods Hole Oceanographic Institution through a Cecil and Ida Green Foundation Innovative Technology Award and an Interdisciplinary Science Award, and a U.S. Environmental Protection Agency (EPA) STAR Graduate Fellowship to J.R.C. under Fellowship Assistance Agreement no. FP-91744301-0. The publication has not been formally reviewed by EPA. The views expressed in this publication are solely those of the authors, and EPA does not endorse any products or commercial services mentioned in this publication.

Availability of data and code

A MATLAB script to read in, process, and estimate rates and uncertainties in dissolved oxygen data from the PHORCYS is provided online at https://github.com/jamesrco/DO_Instruments/. The script can be easily adapted to calculate N_{eff}-based estimates of uncertainty in any dissolved oxygen time series. All PHORCYS and Winkler titration data and other scripts required to reproduce the results and figures in this work are available online in the same location.

Appendix

A new method for calculation of uncertainties in metabolic rate estimates

The ideal means of estimating uncertainties in PHORCYS rates would have been true biological replication, i.e., the simultaneous deployment of several identical instruments in the same water mass. One could then have used the standard deviation of the rate measurements in each different instrument as an estimate of the overall uncertainty. Because we had only one instrument — an exceedingly common situation in oceanographic work — such true replication was not possible. The standard error of the regression slope provides one possible estimate of uncertainty in time-series dissolved oxygen data; for example, this common approach was recently applied to data from *in situ* chamber incubations of sinking marine particle material (McDonnell et al., 2015). However, we assumed that the standard error of regression would significantly underestimate the true uncertainty in our estimates since it does take into account the reduced number of degrees of freedom in such a time series. Because the data points in such a dissolved oxygen time series are not independent of one another, there are almost always far fewer effective degrees of freedom N_{eff} in such data than the number of observations (i.e., data points) N (Emery and Thomson, 2001). (We represent the effective degrees of freedom by the notation N_{eff} in lieu of the N^* notation used by Emery and Thompson.)

Our approach was the following: For each time series of dissolved oxygen concentrations, we first approximated the integral time scale T of the data according to

$$\mathrm{T} = \frac{1}{\mathrm{C}(0)} \int_0^{\mathrm{B}_0} \mathrm{C}(\tau)\,\mathrm{d}\,\tau \qquad \text{(A1)}$$

where $C(0)$ is the value of the autocorrelation function C of the time series at lag $\tau = 0$, and B_0 is the time lag of the autocorrelation function at the first zero crossing of the x-axis, which (after, e.g., Talley et al., 2011) we use as an estimate of the timescale of decorrelation. We then followed the

550 method of Emery and Thompson (2001) to estimate the effective number of degrees of freedom N_{eff}
551 from T, N, and Δt, where Δt is the sampling interval of the data:

552 $$N_{eff} = \frac{N\Delta t}{T} \quad \text{(A2)}$$

553 In this formulation, $N\Delta t$ is therefore the total length of the oxygen time series in which the rate
554 estimate was made. Finally, we used this N_{eff} to obtain $s_{\hat{\beta}_{1,adj}}$, an adjusted estimate of the
555 standardized uncertainty in the slope parameter of the regression (i.e., $\hat{\beta}_1$, the rate of dissolved
556 oxygen consumption or production), according to

557 $$s_{\hat{\beta}_{1,adj}} = \sqrt{\frac{SSE}{N_{eff}-2}\frac{N}{\Delta}} \quad \text{(A3)}$$

558 where SSE is the sum of the squared errors from the fit of the regression, i.e., $\sum_{i=1}^{N}(y_i - \hat{y}_i)^2$, N is
559 the number of observations (as above), and Δ is the determinant $NS_{xx} - S_x^2$. Eq. A3 is simply the
560 formula for calculation of the standard error of the regression slope in the unweighted case, except
561 that N_{eff} is used instead of N.

562 This method of estimating uncertainties in PHORCYS rates produced values of N_{eff}, the
563 number of effective degrees of freedom, which were typically << N, the number of observations in
564 the given dissolved oxygen time series (Table A1). Estimates of the integral time scale T ranged from
565 0.5 to 7.2 h; at station PS-2, the 77.4 h deployment for which data are presented in Fig. 4, we
566 estimated T to be 7.2 h (Table A1). Using the N_{eff} derived from these time scales, we obtained
567 adjusted uncertainty estimates for our PHORCYS rates ($s_{\hat{\beta}_{1,adj}}$) which were much greater in each
568 case than the standard error of the regression slope, $s_{\hat{\beta}_1}$ (compare mean precision of 24.8 % and 3.4
569 %, respectively; Table A1). While more robust than the corresponding $s_{\hat{\beta}_1}$, these $s_{\hat{\beta}_{1,adj}}$ still reflect a

570 fundamental limitation of linear regression: Both methods yield estimates of uncertainty which are
571 inversely proportional to the number of data points (i.e., the length of the underlying data series) and
572 the range of values spanned by the independent variable.

Figures

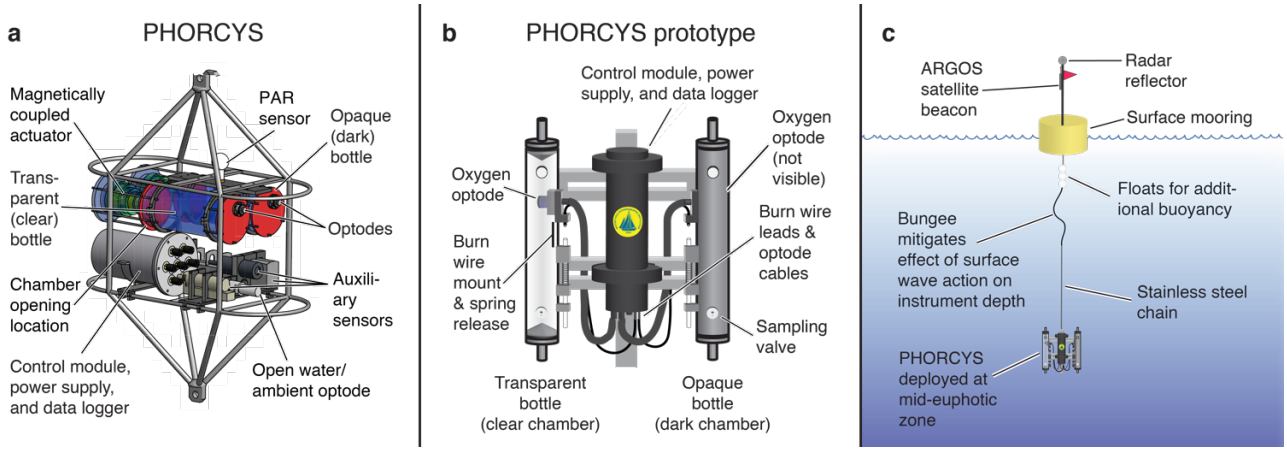

Fig. 1. Design and deployment of the PHORCYS. Major components of the current model PHORCYS and prototype instrument are illustrated in (a) and (b), respectively. (a) The PHORCYS uses magnetically-coupled actuators, allowing for multiple openings and closings of the chambers during a single deployment. The current instrument also includes several sensors for collection of auxiliary data in the water outside of the chamber, including photosynthetically active radiation (PAR), conductivity, ambient temperature, transmissivity, and chlorophyll fluorescence. The PHORCYS also includes a third optode to measure dissolved oxygen concentrations in the ambient water mass outside of the two chambers. (c) Rigging scheme for open-ocean deployments from a drifting surface mooring, as described in the text.

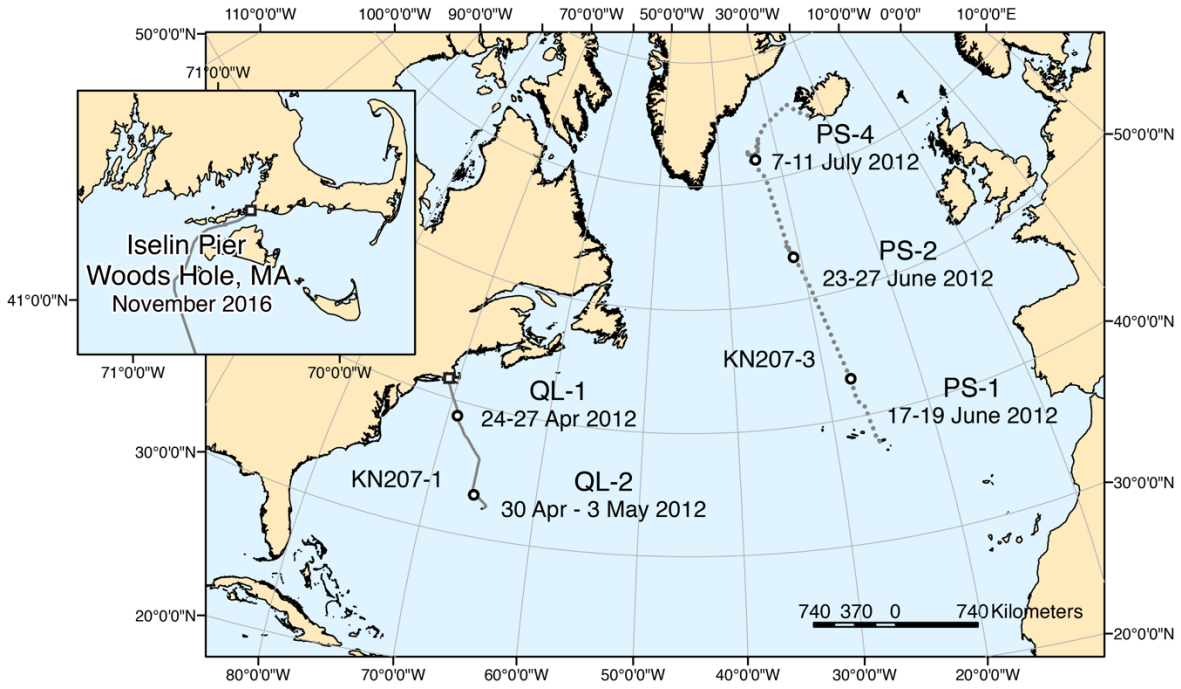

584

585 **Fig. 2.** Locations of PHORCYS deployments described in the text. Primary map: Unattended open-
586 ocean deployments from a surface mooring were conducted using the PHORCYS prototype at 5
587 stations during two cruises aboard the *R/V Knorr*. Stations QL-1 and QL-2 were conducted during
588 cruise KN207-1; PS-1, PS-2, and PS-3 were conducted during cruise KN207-3. Inset: Pierside
589 deployments using the present PHORCYS model were conducted in November 2016 at the Iselin
590 Marine Facility in Woods Hole, MA, USA.

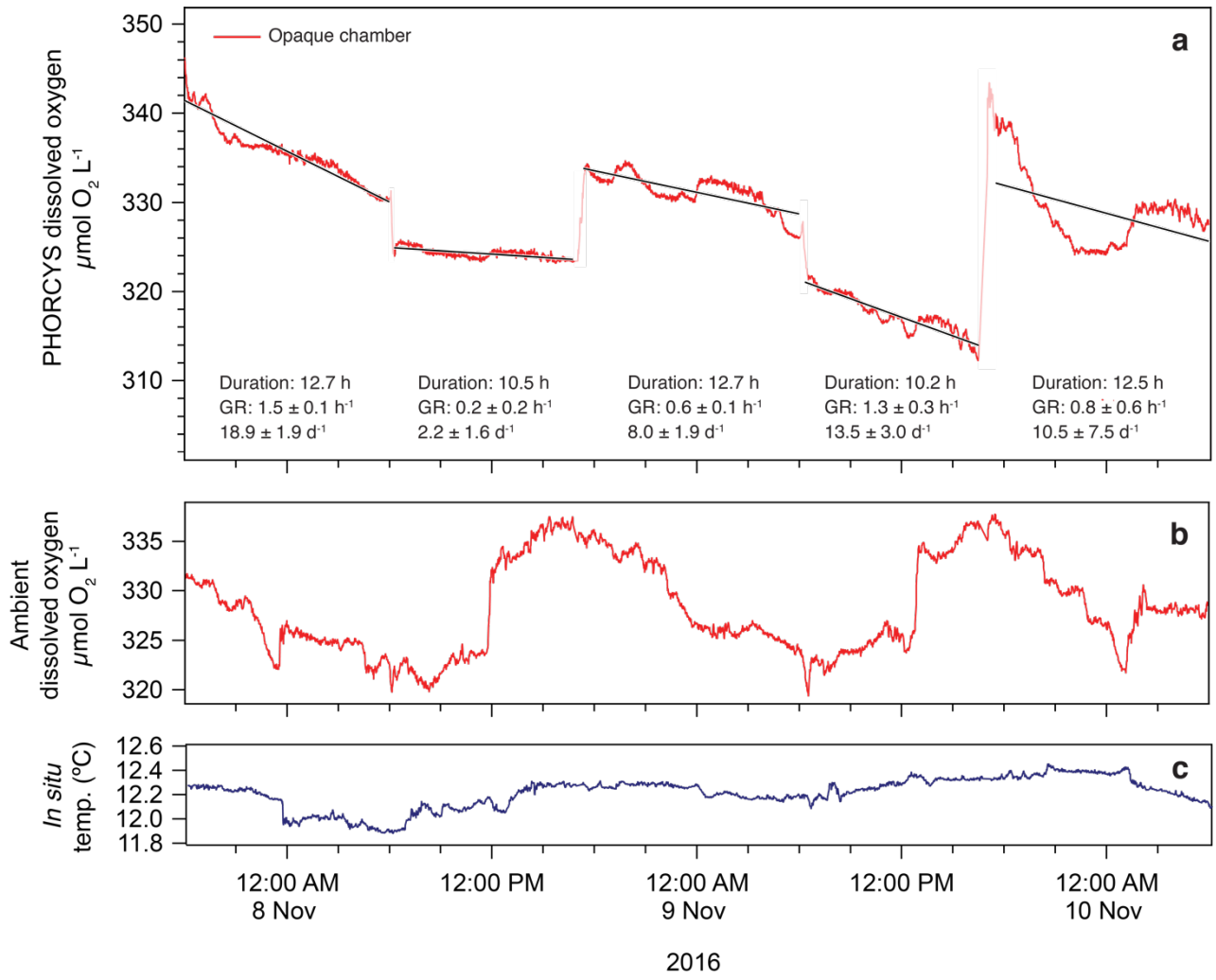

591

592 **Fig. 3.** Continuous, unattended observations of community respiration at the Iselin Pier in Woods
593 Hole over a 3 d period in November 2016. (a) Record of dissolved oxygen concentration in the
594 opaque PHORCYS chamber. The incubation periods from which estimates of GR were calculated are
595 separated by 30 min, *in situ* flushing periods when the chamber was opened and closed to obtain a
596 new water sample. Separate estimates of GR for each of the incubation periods (units of µmol O_2 L^{-1}
597 d^{-1}) were obtained by linear least-squares regression, and are shown as solid traces superimposed
598 over the instrument data; these are the Iselin Pier data reported in Tables 2 and A1. Uncertainties
599 were determined using the effective degrees of freedom method described in the Appendix. (b)
600 Ambient *in situ* dissolved oxygen concentration measured concurrently outside the PHORCYS
601 chambers, reflecting tidal changes in water-mass properties. (c) Ambient *in situ* temperature data

recorded outside the PHORCYS chambers. An instrument malfunction during the deployment prevented us from recovering data from the transparent PHORCYS chamber.

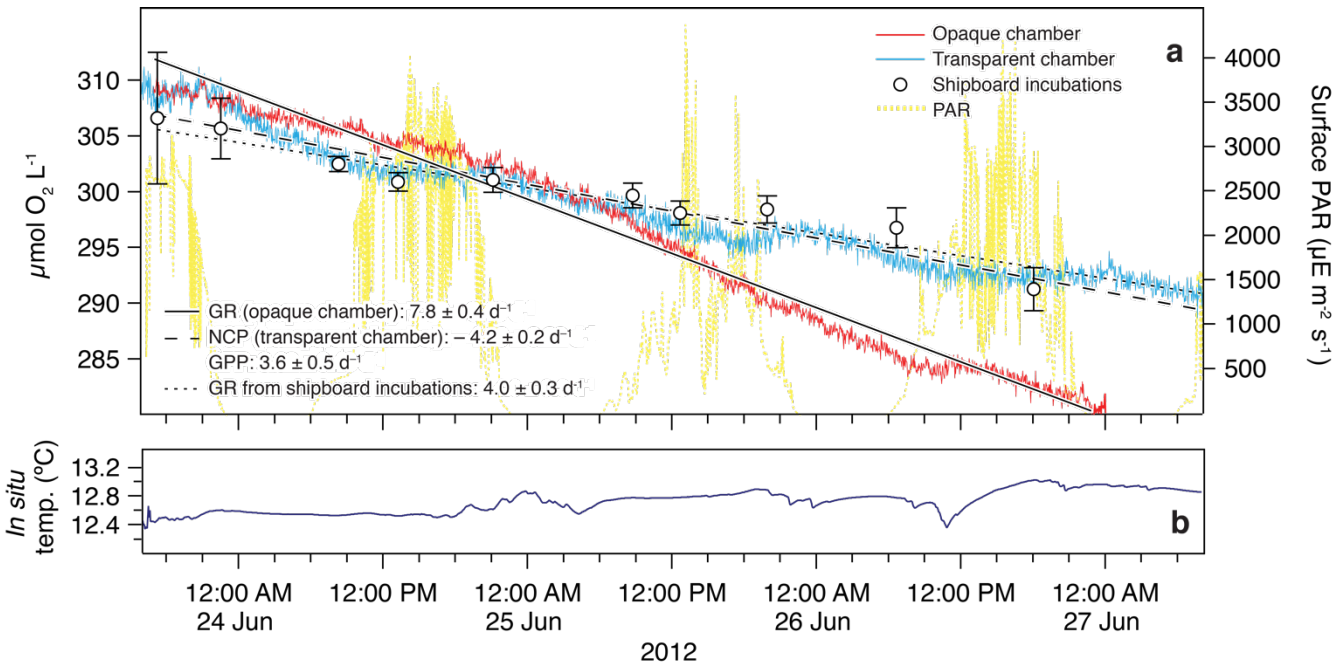

604

605 **Fig. 4.** Unattended observations of ecosystem metabolism made with the prototype PHORCYS
606 instrument at station PS-2 (Fig. 2; Supplemental Table 1) during a sub-Arctic, open-ocean
607 deployment aboard the R/V *Knorr*. A midsummer bloom of a calcifying phytoplankton species was
608 in progress at the site (Collins et al., 2015) when these observations were made. (a) Estimates (in
609 units of μmol O_2 L^{-1} d^{-1}) of gross community respiration (GR) and net community production (NCP)
610 were obtained by linear least-squares regression, and are shown as traces (GR as solid trace; NCP as
611 dashed trace) superimposed over the instrument data. The prototype instrument allowed for only a
612 single incubation over the course of the deployment. GPP was calculated as the difference between
613 GR and NCP based on Eq. 4 in the text. Uncertainties were determined using the effective degrees of
614 freedom method described in the Appendix. Incident photosynthetically active radiation (PAR) was
615 measured using shipboard sensors. Dissolved oxygen concentrations measured concurrently in dark
616 shipboard incubations using optode sensor spots (5 replicates; error bars show ± SD) are
617 superimposed as open circles. The respiration rate estimated from these incubations is shown as a
618 dotted trace. (b) Diel warming of the surface layer is evident in *in situ* temperature data collected by
619 the PHORCYS.

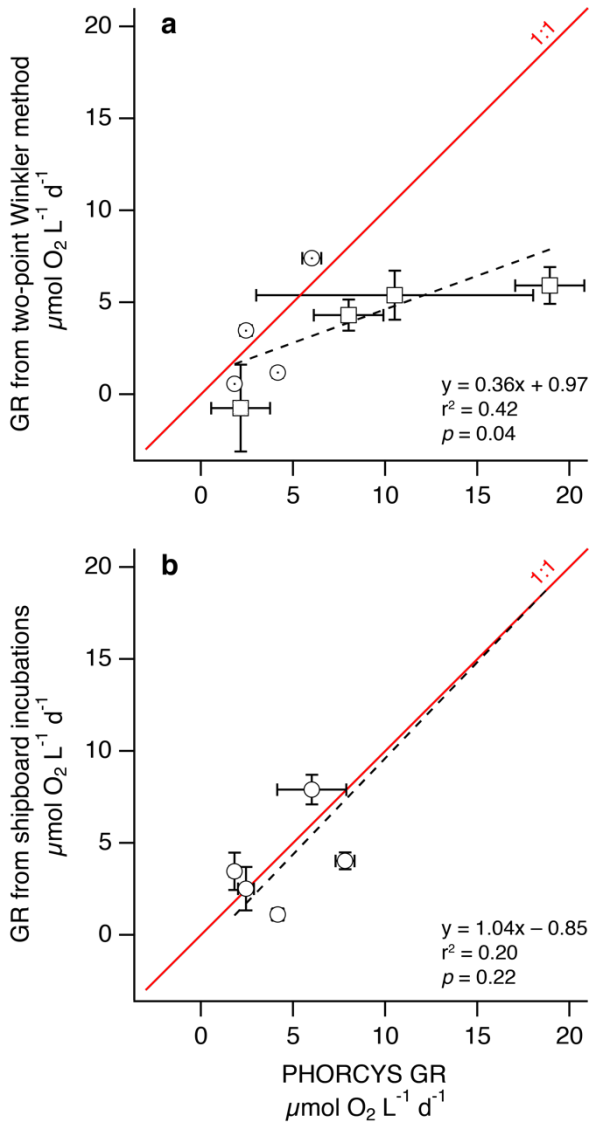

620

621 **Fig. 5.** Comparison of community respiration (GR) rate estimates from the PHORCYS (*x*-axis) with
622 rates determined by (a) the two-point Winkler titration method and (b) a series of shipboard bottle
623 incubations using optode sensor spots. Circles show data from the prototype instrument, while
624 squares show data collected with the present PHORCYS model. A Type II (major axis) regression
625 (dashed line) was fit to each set of paired observations using the lmodel2 package for R (Legendre,
626 2014). In (a), the regression model was fit to a single dataset consisting of both current and prototype
627 model data. A red 1:1 line is superimposed in each panel for reference.

628

Table 1. Estimated surface area to volume ratios of PHORCYS chambers and standard BOD bottles.

Bottle or chamber type	Actual usable volume (mL)	Estimated internal surface area (cm^2)	Estimated surface area : volume ratio
PHORCYS chamber (prototype)	2610	1760	0.67
PHORCYS chamber (current model)	5680	2035	0.34
Typical 125 mL BOD bottle	149.2 ± 0.3	124.4 ± 5.0	0.83
Typical 300 mL BOD bottle	299.2 ± 0.4	229.1 ± 4.3	0.77

The average volumes and surface areas reported in this table for BOD bottles were determined from independent measurements of the dimensions of 10 different bottles of each size; these were chosen at random from the Woods Hole Oceanographic Institution inventory.

635 **Table 2.** Rates of community respiration measured in opaque bottles using the PHORCYS and two independent, traditional methods.

Deployment dates	Incubation period	Incubation duration (h)	Location[a]	PHORCYS model[b]	Community respiration (GR) (μmol O_2 L^{-1} d^{-1} ± uncertainty)		
					PHORCYS opaque bottle[c]	Shipboard incubations[d]	Two-point difference of Winkler titrations at *t*=0 and recovery[e]
24-27 Apr 2012	Entire deployment	71.6	QL-1	Prototype	1.8 ± 0.2	3.2 ± 0.7	0.6 ± 0.1
30 Apr - 3 May 2012	Entire deployment	65.4	QL-2	Prototype	4.2 ± 0.3	1.1 ± 0.2	1.2 ± 0.04
17-19 June 2012	Entire deployment	41.2	PS-1	Prototype	2.4 ± 0.3	3.4 ± 0.5	3.5 ± 0.2
23-27 June 2012	Entire deployment	77.4	PS-2	Prototype	7.8 ± 0.4	4.0 ± 0.3	—
7-11 July 2012	Entire deployment	94.0	PS-4	Prototype	6.0 ± 0.5	7.9 ± 0.6	7.4 ± 0.2
7-8 Nov 2016	17:15-06:00	12.7	Iselin Pier	Present model	18.9 ± 1.9	—	5.9 ± 1.0
8 Nov 2016	06:15-16:45	10.5	Iselin Pier	Present model	2.2 ± 1.6	—	–0.8 ± 2.4
8-9 Nov 2016	17:20-06:00	12.7	Iselin Pier	Present model	8.0 ± 1.9	—	4.3 ± 0.9
9-10 Nov 2016	17:30-06:00	12.5	Iselin Pier	Present model	10.5 ± 7.5	—	5.4 ± 1.3

636
637 [a] Cruise station or geographical location (Fig. 2); additional metadata for each station are provided in Supplemental Table 1
638 [a] See Fig. 1
639 [c] Uncertainty adjusted for effective degrees of freedom, as described in the Appendix
640 [d] Mean of ≥ 5 replicates; uncertainty derived from standard error of regression slope
641 [e] Mean of 3 replicates; uncertainty derived from standard error

Table A1. Comparison of methods for estimation of uncertainties in dissolved oxygen time series data.

Deployment dates	Location[a]	PHORCYS community respiration (GR) (µmol O_2 L^{-1} d^{-1})	No. obser-vations (*N*)	Incubation duration (h)	Est. integral time scale (h)	Effective degrees of freedom (N_{eff})	Estimated uncertainty (µmol O_2 L^{-1} d^{-1})		Method precision (est. uncertainty as percent of rate measurement)	
							Standard error of regression slope ($s_{\hat{\beta}_1}$)	Adjusted estimate $s_{\hat{\beta}_{1,adj}}$ based on N_{eff}	$s_{\hat{\beta}_1}$	$s_{\hat{\beta}_{1,adj}}$
24-27 Apr 2012	QL-1	1.8	2150	71.6	1.1	66.5	0.03	0.18	1.6 %	9.9 %
30 Apr - 3 May 2012	QL-2	4.2	1964	65.4	3.1	21.0	0.03	0.28	0.7 %	6.7 %
17-19 June 2012	PS-1	2.4	1238	41.2	0.5	76.4	0.08	0.32	3.3 %	13.1 %
23-27 June 2012	PS-2	7.8	2323	77.4	7.2	10.7	0.03	0.43	0.4 %	5.5 %
7-11 July 2012	PS-4	6.0	2820	94.0	1.9	49.8	0.07	0.52	1.2 %	8.6 %
7-8 Nov 2016	Iselin Pier	18.9	765	12.7	1.3	19.8	0.29	1.87	1.5 %	9.9 %
8 Nov 2016	Iselin Pier	2.2	627	10.5	1.2	17.0	0.25	1.60	11.6 %	74.4 %
8-9 Nov 2016	Iselin Pier	8.0	760	12.7	1.6	16.2	0.26	1.89	3.2 %	23.6 %
9-10 Nov 2016	Iselin Pier	10.5	750	12.5	2.9	8.7	0.71	7.51	6.7 %	71.4 %
Mean					2.3				3.4 %	24.8 %

[a] Cruise station or geographical location (Fig. 2); additional metadata for each station are provided in Supplemental Table 1

649 **References**
650

651 Anderson, L.A., and Sarmiento, J.L. 1994. Redfield ratios of remineralization determined by nutrient
652 data-analysis. *Global Biogeochemical Cycles* 8, 65-80.

653 Aranguren-Gassis, M., Serret, P., Fernández, E., Herrera, J.L., Domínguez, J.F., Pérez, V., and
654 Escanez, J. 2012. Balanced plankton net community metabolism in the oligotrophic North Atlantic
655 subtropical gyre from Lagrangian observations. *Deep Sea Research Part I: Oceanographic Research*
656 *Papers* 68, 116-122.

657 Belcher, A., Iversen, M., Giering, S., Riou, V., Henson, S.A., Berline, L., Guilloux, L. and Sanders,
658 R. 2016a. Depth-resolved particle-associated microbial respiration in the northeast Atlantic.
659 *Biogeosciences* 13, 4927-4943.

660 Belcher, A., Iversen, M., Manno, C., Henson, S.A., Tarling, G.A. and Sanders, R. 2016b. The role of
661 particle associated microbes in remineralization of fecal pellets in the upper mesopelagic of the
662 Scotia Sea, Antarctica. *Limnology and Oceanography* 61, 1049-1064.

663 Bender, M., Grande, K., Johnson, K., Marra, J., Williams, P.J., Sieburth, J., Pilson, M., Langdon, C.,
664 Hitchcock, G., Orchardo, J., Hunt, C., Donaghay, P., and Heinemann, K. 1987. A comparison of 4
665 methods for determining planktonic community production. *Limnology and Oceanography* 32, 1085-
666 1098.

667 Bender, M., Orchardo, J., Dickson, M.-L., Barber, R., and Lindley, S. 1999. *In vitro* O_2 fluxes
668 compared with ^{14}C production and other rate terms during the JGOFS Equatorial Pacific experiment.
669 *Deep Sea Research Part I: Oceanographic Research Papers* 46, 637-654.

670 Boyd, P.W., McDonnell, A., Valdez, J., Lefevre, D., and Gall, M.P. 2015. RESPIRE: An *in situ*
671 particle interceptor to conduct particle remineralization and microbial dynamics studies in the
672 oceans' Twilight Zone. *Limnology and Oceanography: Methods* 13, 494-508.

673 Caffrey, J. 2004. Factors controlling net ecosystem metabolism in U.S. estuaries. *Estuaries and*
674 *Coasts* 27, 90-101.

675 Calvo-Díaz, A., Díaz-Pérez, L., Suárez, L.Á., Morán, X.a.G., Teira, E., and Marañón, E. 2011.
676 Decrease in the autotrophic-to-heterotrophic biomass ratio of picoplankton in oligotrophic marine
677 waters due to bottle enclosure. *Applied and Environmental Microbiology* 77, 5739-5746.

678 Collins, J.R., Edwards, B.R., Thamatrakoln, K., Ossolinski, J.E., Ditullio, G.R., Bidle, K.D., Doney,
679 S.C., and Van Mooy, B.A.S. 2015. The multiple fates of sinking particles in the North Atlantic
680 Ocean. *Global Biogeochemical Cycles* 29, 1471-1494.

681 Collins, J.R., Raymond, P.A., Bohlen, W.F., and Howard-Strobel, M.M. 2013. Estimates of new and
682 total productivity in Central Long Island Sound from *in situ* measurements of nitrate and dissolved
683 oxygen. *Estuaries and Coasts* 36, 74–97.

684 Dang, H. and Lovell, C.R. 2016. Microbial surface colonization and biofilm development in marine
685 environments. *Microbiol. Mol. Biol. Rev*. 80, 91-138.

686 Del Giorgio, P.A., and Williams, P.J. 2005. *Respiration in Aquatic Ecosystems.* Oxford, U.K.:
687 Oxford University Press.

688 Del Giorgio, P.A., and Pace, M.L. 2008. Relative independence of organic carbon transport and
689 processing in a large temperate river: The Hudson River as both pipe and reactor. *Limnol. Oceanogr.*
690 53, 185-197.

691 Delauney, L., Compère, C., and Lehaitre, M. 2010. Biofouling protection for marine environmental
692 sensors. Ocean Science 6, 503-511.

693 Denman, K.L., Brasseur, G., Chidthaisong, A., Ciais, P., Cox, P.M., Dickinson, R.E., Hauglustaine,
694 D., Heinze, C., Holland, E., Jacob, D., Lohmann, U., Ramachandran, S., Da Silva Dias, P.L., Wofsy,
695 S.C., and Zhang, X. 2007. "Couplings between changes in the climate system and biogeochemistry,"
696 in *Climate Change 2007: The Physical Science Basis. Contribution of Working Group I to the Fourth*
697 *Assessment Report of the Intergovernmental Panel on Climate Change,* eds. S. Solomon, D. Qin, M.
698 Manning, Z. Chen, M. Marquis, K.B. Averyt, T. M. & H.L. Miller. (Cambridge, U.K.: Cambridge
699 University Press), 89 p.

700 Duarte, C.M., Regaudie-De-Giroux, A., Arrieta, J.M., Delgado-Huertas, A., and Agustí, S. 2013. The
701 oligotrophic ocean is heterotrophic. *Annual Review of Marine Science* 5, 18.11–18.19.

702 Ducklow, H.W., and Doney, S.C. 2013. What is the metabolic state of the oligotrophic ocean? A
703 debate. *Annual Review of Marine Science* 5, 15.11–15.19.

704 Edwards, B.R., Reddy, C.M., Camilli, R., Carmichael, C.A., Longnecker, K., and Van Mooy, B.A.S.
705 2011. Rapid microbial respiration of oil from the Deepwater Horizon spill in offshore surface waters
706 of the Gulf of Mexico. *Environmental Research Letters* 6.

707 Emery, W.J., and Thomson, R.E. 2001. *Data Analysis Methods in Physical Oceanography.*
708 Amsterdam: Elsevier Science.

709 Figueroa, F.L., Mercado, J.M., Beardall, J., Neale, P.J., Montecino, V. and Kromkamp, J.C. 2014.
710 Introduction. *Aquatic Biology* 22, 1-4.

711 Fogg, G.E., and Calvario-Martinez, O. 1989. Effects of bottle size in determinations of primary
712 productivity by phytoplankton. *Hydrobiologia* 173, 89-94.

713 Fuchsman, C.A., Devol, A.H., Chase, Z., Reimers, C.E., and Hales, B. 2015. Benthic fluxes on the
714 Oregon shelf. *Estuarine, Coastal and Shelf Science* 163, Part B, 156-166.

715 Furnas, M.J. 2002. "Measuring the growth rates of phytoplankton in natural populations," in *Pelagic*
716 *Ecology Methodology,* ed. D.V.S. Rao. (Lisse: A. A. Balkema Publishers), 221-249.

717 Gaarder, T., and Gran, H.H. 1927. Investigations of the production of plankton in the Oslo Fjord.
718 *Rapports et Procès-Verbaux des Réunions du Conseil Permanent International pour l'Exploration de*
719 *la Mer* 42, 1-48.

720 Goldman, J.A.L., Kranz, S.A., Young, J.N., Tortell, P.D., Stanley, R.H.R., Bender, M.L., and Morel,
721 F.M.M. 2015. Gross and net production during the spring bloom along the Western Antarctic
722 Peninsula. *New Phytologist* 205, 182-191.

723 Guillemette, F., and del Giorgio, P.A. 2011. Reconstructing the various facets of dissolved organic
724 carbon bioavailability in freshwater ecosystems. *Limnol. Oceanogr.* 56, 734-748.

725 Guillemette, F., McCallister, S.L., and del Giorgio, P.A. 2013. Differentiating the degradation
726 dynamics of algal and terrestrial carbon within complex natural dissolved organic carbon in
727 temperate lakes. *Journal of Geophysical Research: Biogeosciences* 118, 963-973.

728 Hammond, D.E., Cummins, K.M., Mcmanus, J., Berelson, W.M., Smith, G., and Spagnoli, F. 2004.
729 Methods for measuring benthic nutrient flux on the California Margin: Comparing shipboard core
730 incubations to *in situ* lander results. *Limnology and Oceanography: Methods* 2, 146-159.

731 Karl, D.M., Dore, J.E., and Paul, J.H. 2001. "Microbial ecology at sea: Sampling, subsampling and
732 incubation considerations," in *Methods in Microbiology,* ed. J.H. Paul. (Waltham, MA, USA:
733 Academic Press), 13-39.

734 Kenner, R.A., and Ahmed, S.I. 1975. Measurements of electron transport activities in marine
735 phytoplankton. *Marine Biology* 33, 119-127.

736 Kim, S.-H., Choi, A., Jin Yang, E., Lee, S., and Hyun, J.-H. 2016. Low benthic respiration and
737 nutrient flux at the highly productive Amundsen Sea Polynya, Antarctica. *Deep Sea Research Part*
738 *II: Topical Studies in Oceanography* 123, 92-101.

739 Kjeldsen, P. 1993. Evaluation of gas diffusion through plastic materials used in experimental and
740 sampling equipment. *Water Research* 27, 121-131.

741 Klimant, I., Meyer, V., and Kühl, M. 1995. Fiber-optic oxygen microsensors, a new tool in aquatic
742 biology. *Limnology and Oceanography* 40, 1159-1165.

743 Knapp, G.P., Stalcup, M.C., and Stanley, R.J. 1989. "Dissolved oxygen measurements in sea water at
744 the Woods Hole Oceanographic Institution." Report WHOI-89-23. Woods Hole, MA: Woods Hole
745 Oceanographic Institution, 18 p.

746 Langdon, C., Marra, J., and Knudson, C. 1995. Measurements of net and gross O_2 production, dark
747 O_2 respiration, and ^{14}C assimilation at the Marine Light-Mixed Layers site (59°N, 21°W) in the
748 northeast Atlantic Ocean. *Journal of Geophysical Research: Oceans* 100, 6645-6653.

749 Lee, J.S., An, S.-U., Park, Y.-G., Kim, E., Kim, D., Kwon, J.N., Kang, D.-J., and Noh, J.-H. 2015.
750 Rates of total oxygen uptake of sediments and benthic nutrient fluxes measured using an *in situ*
751 autonomous benthic chamber in the sediment of the slope off the southwestern part of Ulleung Basin,
752 East Sea. *Ocean Science Journal* 50, 581-588.

753 Legendre, P. 2014. "lmodel2: Model II Regression." R package, version 1.7-2.

754 Manov, D.V., Chang, G.C., and Dickey, T.D. 2004. Methods for reducing biofouling of moored
755 optical sensors. Journal of Atmospheric and Oceanic Technology 21, 958-968.

756 Martens, C.S., Mendlovitz, H.P., Seim, H., Lapham, L., and D'Emidio, M. 2016. Sustained *in situ*
757 measurements of dissolved oxygen, methane and water transport processes in the benthic boundary
758 layer at MC118, northern Gulf of Mexico. *Deep Sea Research Part II: Topical Studies in*
759 *Oceanography* 129, 41-52.

760 McDonnell, A.M.P., Boyd, P.W., and Buesseler, K.O. 2015. Effects of sinking velocities and
761 microbial respiration rates on the attenuation of particulate carbon fluxes through the mesopelagic
762 zone. *Global Biogeochemical Cycles* 29, 2014GB004935.

763 Moore, C., Barnard, A., Fietzek, P., Lewis, M.R., Sosik, H.M., White, S., and Zielinski, O. 2009.
764 Optical tools for ocean monitoring and research. *Ocean Science* 5, 661-684.

765 Nicholson, D.P., Wilson, S.T., Doney, S.C., and Karl, D.M. 2015. Quantifying subtropical North
766 Pacific gyre mixed layer primary productivity from Seaglider observations of diel oxygen cycles.
767 *Geophysical Research Letters* 42, 4032-4039.

768 Porter, J.H., Nagy, E., Kratz, T.K., Hanson, P., Collins, S.L., and Arzberger, P. 2009. New eyes on
769 the world: Advanced sensors for ecology. *Bioscience* 59, 385-397.

770 Pratt, D.M. and Berkson, H. 1959. Two sources of error in the oxygen light and dark bottle method.
771 *Limnology and Oceanography* 4, 328-334.

772 Prien, R.D. 2007. The future of chemical *in situ* sensors. *Marine Chemistry* 107, 422-432.

773 Quay, P.D., Peacock, C., Björkman, K., and Karl, D.M. 2010. Measuring primary production rates in
774 the ocean: Enigmatic results between incubation and non-incubation methods at Station ALOHA.
775 *Global Biogeochem. Cycles* 24, GB3014.

776 Redfield, A.C. 1934. "On the proportions of organic derivatives in sea water and their relation to the
777 composition of plankton," in *James Johnstone Memorial Volume,* ed. R.J. Daniel. University Press of
778 Liverpool), 176-192.

779 Regaudie-De-Gioux, A., Lasternas, S., Agustí, S., and Duarte, C.M. 2014. Comparing marine
780 primary production estimates through different methods and development of conversion equations.
781 *Frontiers in Marine Science* 1.

782 Reinthaler, T., Van Aken, H.M., and Herndl, G.J. 2010. Major contribution of autotrophy to
783 microbial carbon cycling in the deep North Atlantic's interior. *Deep-Sea Research Part II-Topical*
784 *Studies in Oceanography* 57, 1572-1580.

785 Riser, S.C., and Johnson, K.S. 2008. Net production of oxygen in the subtropical ocean. *Nature* 451,
786 323-U325.

787 Robert, A. 2012. Mineralisation *in situ* de la matière organique le long de la colonne d'eau:
788 Application sur une station eulerienne. Dissertation. Marseille: Université d'Aix-Marseille.

789 Robinson, C., and Williams, P.J. 2005. "Respiration and its measurement in surface marine waters,"
790 in *Respiration in Aquatic Ecosystems,* eds. P. Del Giorgio & P.J. Williams. (New York: Oxford
791 University Press).

792 Robinson, C., Tilstone, G.H., Rees, A.P., Smyth, T.J., Fishwick, J.R., Tarran, G.A., Luz, B., Barkan,
793 E., and David, E. 2009. Comparison of *in vitro* and *in situ* plankton production determinations.
794 *Aquatic Microbial Ecology* 54, 13-34.

795 Salta, M., Wharton, J.A., Blache, Y., Stokes, K.R. and Briand, J.-F. 2013. Marine biofilms on
796 artificial surfaces: structure and dynamics. *Environ. Microbiol*. 15, 2879-2893.

797 Spanjers, H., Olsson, G., and Klapwijk, A. 1994. Determining short-term biochemical oxygen
798 demand and respiration rate in an aeration tank by using respirometry and estimation. *Water*
799 *Research* 28, 1571-1583.

800 Staehr, P.A., Testa, J.M., Kemp, W.M., Cole, J.J., Sand-Jensen, K., and Smith, S.V. 2012. The
801 metabolism of aquatic ecosystems: history, applications, and future challenges. *Aquatic Sciences* 74,
802 15-29.

803 Steeman Nielsen, E. 1952. The use of radioactive carbon (^{14}C) for measuring organic production in
804 the sea. *Journal du Conseil - Conseil International pour l'Exploration de la Mer* 18, 117-140.

805 Stumm, W., and Morgan, J.J. 2013. *Aquatic Chemistry: Chemical Equilibria and Rates in Natural*
806 *Waters.* New York: Wiley.

807 Suter, E.A., Scranton, M.I., Chow, S., Stinton, D., Medina Faull, L., and Taylor, G.T. 2016. Niskin
808 bottle sample collection aliases microbial community composition and biogeochemical interpretation.
809 *Limnology and Oceanography*. doi: 10.1002/lno.10447

810 Talley, L.D., Pickard, G.L., Emery, W.J., and Swift, J.H. 2011. "Data analysis concepts and
811 observational methods," in *Descriptive Physical Oceanography*. 6th ed (Boston: Academic Press),
812 147-186.

813 Tamburini, C., Boutrif, M., Garel, M., Colwell, R.R., and Deming, J.W. 2013. Prokaryotic responses
814 to hydrostatic pressure in the ocean – a review. *Environmental Microbiology* 15, 1262-1274.

815 Taylor, C.D., and Doherty, K.W. 1990. Submersible Incubation Device (SID), autonomous
816 instrumentation for the *in situ* measurement of primary production and other microbial rate processes.
817 *Deep-Sea Research Part A-Oceanographic Research Papers* 37, 343-358.

818 Taylor, C.D., Howes, B.L., and Doherty, K.W. 1993. Automated instrumentation for time-series
819 measurement of primary production and nutrient status in production platform-accessible
820 environments. *Marine Technology Society Journal* 27, s32-44.

821 Tengberg, A., Hovdenes, J., Andersson, H.J., Brocandel, O., Diaz, R., Hebert, D., Arnerich, T.,
822 Huber, C., Körtzinger, A., Khripounoff, A., Rey, F., Rönning, C., Schimanski, J., Sommer, S., and
823 Stangelmayer, A. 2006. Evaluation of a lifetime-based optode to measure oxygen in aquatic systems.
824 *Limnology and Oceanography: Methods* 4, 7-17.

825 Venrick, E.L., Beers, J.R., and Heinbokel, J.F. 1977. Possible consequences of containing
826 microplankton for physiological rate measurements. *Journal of Experimental Marine Biology and*
827 *Ecology* 26, 55-76.

828 Volkmar, E.C., and Dahlgren, R.A. 2006. Biological oxygen demand dynamics in the Lower San
829 Joaquin River, California. *Environmental Science & Technology* 40, 5653-5660.

830 Wang, Z.A., Sonnichsen, F.N., Bradley, A.M., Hoering, K.A., Lanagan, T.M., Chu, S.N., Hammar,
831 T.R., and Camilli, R. 2015. *In situ* sensor technology for simultaneous spectrophotometric

measurements of seawater total dissolved inorganic carbon and pH. *Environmental Science & Technology* 49, 4441-4449.

Warkentin, M., Freese, H.M., Karsten, U., and Schumann, R. 2007. New and fast method to quantify respiration rates of bacterial and plankton communities in freshwater ecosystems by using optical oxygen sensor spots. *Applied and Environmental Microbiology* 73, 6722-6729.

Wikner, J., Panigrahi, S., Nydahl, A., Lundberg, E., Båmstedt, U., and Tengberg, A. 2013. Precise continuous measurements of pelagic respiration in coastal waters with Oxygen Optodes. *Limnology and Oceanography: Methods* 11, 1-15

Williams, P.J. 1998. The balance of plankton respiration and photosynthesis in the open oceans. *Nature* 394, 55-57.

Williams, P.J., Quay, P.D., Westberry, T.K., and Behrenfeld, M.J. 2013. The oligotrophic ocean is autotrophic. *Annual Review of Marine Science* 5, 16.11-16.15.

Winkler, L.W. 1888. Die Bestimmung des im Wasser gelosten Sauerstoffes. *Ber. Dtsch. Chem. Ges. Berlin* 21, 2843-2846.

Yvon-Durocher, G., Caffrey, J.M., Cescatti, A., Dossena, M., Giorgio, P.D., Gasol, J.M., Montoya, J.M., Pumpanen, J., Staehr, P.A., Trimmer, M., Woodward, G., and Allen, A.P. 2012. Reconciling the temperature dependence of respiration across timescales and ecosystem types. *Nature* 487, 472-476.